Materials Research
Express

INCLUSIVE PUBLISHING
TRUSTED SCIENCE

PURPOSE-LED
PUBLISHING™

PAPER

MoO_3 nanoparticle anchored graphene as bifunctional agent for water purification

To cite this article: Homen Lahan *et al* 2016 *Mater. Res. Express* **3** 105003

View the article online for updates and enhancements.

You may also like

- Improved photocatalytic degradation of methylene blue and rhodamine G dye under UV-radiation by rGO-MoO_3
  Ruhinaz Ushal, Bilal Ahmed, Arvind Singh et al.
- Efficient non-fullerene organic solar cells employing aqueous solution-processed MoO_3 as a hole-transporting layer
  Yaozhao Li, Peng Li, Minghao Qu et al.
- A facile one pot synthesis of MoO_3 on reduced graphene oxide (RGO) and electrochemical studies for energy applications
  Krishnamurthy G and Veeresha G


UNITED THROUGH SCIENCE & TECHNOLOGY

The Electrochemical Society
Advancing solid state & electrochemical science & technology

248th
ECS Meeting
Chicago, IL
October 12-16, 2025
Hilton Chicago

Science +
Technology +
YOU!

SUBMIT
ABSTRACTS by
March 28, 2025

SUBMIT NOW

This content was downloaded from IP address 165.123.34.86 on 24/01/2025 at 20:47

IOP Publishing Mater. Res. Express 3 (2016) 105003 doi:10.1088/2053-1591/3/10/105003

Materials Research Express

RECEIVED
27 January 2016

REVISED
5 March 2016

ACCEPTED FOR PUBLICATION
18 April 2016

PUBLISHED
7 October 2016

PAPER

MoO_3 nanoparticle anchored graphene as bifunctional agent for water purification

Homen Lahan[1], **Raju Roy**[2], **Nima D Namsa**[2] **and Shyamal K Das**[1]

[1] Department of Physics, Tezpur University, Assam, India, 784028
[2] Department of Molecular Biology and Biotechnology, Tezpur University, Assam, India, 784028

E-mail: namsa@tezu.ernet.in and skdas@tezu.ernet.in

Keywords: graphene, MoO_3, nanocomposites, adsorption

Abstract

We report here a facile one step hydrothermal method to anchor MoO_3 nanoparticles in graphene. The bifunctionality of graphene-MoO_3 nanoparticles is demonstrated via dye adsorption and antibacterial activities. The nanocomposite showed excellent adsorption of methylene blue, a cationic dye, from water compared to pristine MoO_3 and graphene. However, it showed negligible adsorption of methyl orange, an anionic dye. Again, the graphene-MoO_3 nanoparticles exhibited bacteriostatic property against both Gram-negative (*E. coli*) and Gram-positive (*S. aureus*) bacteria.

1. Introduction

A major global challenge, mostly in developing countries, is to sustain clean and pure water with rapid industrialization, population growth and exponential improvements in living standards. It is apparent that the natural water resources are often contaminated by waste organic/inorganic materials and pathogens originating from unavoidable human activities. Therefore, there is a growing need for affordable technologies for water preservation and purification.

Synthetic dyes wasted from various industries are most notable examples of organic pollutants in water [1–5]. Large quantities of different types of synthetic dyes ($\sim10^6$ tons in a year) are produced globally and nearly 1.5×10^5 tons are released into the environment (mostly in water bodies) as waste [1–5]. This situation is more alarming in countries like China and India where the consumption rate of dyes are higher. It amounts to ~40%–45% and ~10% of global consumption for China and India respectively [4, 5]. Removal of these waste dye pollutants from water is vital for the protection of the ecosystem. One widely used technique for this purpose is adsorption [6, 7]. Inorganic materials have been extensively investigated for effective adsorption of dyes from water [6–17]. Although these materials showed excellent adsorption properties, their activity is limited in killing or inhibiting pathogenic growth [18]. Therefore, it would be extraordinary if the adsorption material shows antimicrobial activities so that it acts as a bifunctional agent for water purification. Reports on bifunctional materials are sporadic in this context [6, 19, 20]. One example of such bifunctional material found in the literature is Ag_2WO_4 [19, 20]. Dutta *et al* reported utilization of Ag_2WO_4 nanorods for adsorption of various cationic dyes and also demonstrated the bactericidal effect against both gram-negative and gram-positive bacterial strains [19]. Later on, Roca *et al* combined both experimental and theoretical methods to explain the facet-dependent photocatalytic and antibacterial properties of Ag_2WO_4 crystals [20]. Therefore, bifunctional materials need global attention and there is an urgent need to explore other novel materials that demonstrate both these activities simultaneously. One such material example may be molybdenum trioxide (MoO_3). MoO_3 is an important class of transition metal oxides having its application in wide verity of areas such as optical, electrochemical, electronics and sensors applications [21–29]. However, there are very limited reports on the direct adsorption properties of MoO_3 [30, 31]. Ma *et al* explored the possibility of adsorption of methylene blue (MB) dye by MoO_3 nanobelts [30]. Wang *et al* demonstrated selective adsorption of organic dyes by 3D hierarchical architecture of MoO_3 [31]. It is also noted here that there are only few examples of photodegradation of organic dyes by MoO_3 [32–39]. Similarly, very few reports are available on the antimicrobial properties of MoO_3 [40–42]. Surprisingly, to the best of our knowledge, there are no reports so far

© 2016 IOP Publishing Ltd

where both organic dye adsorption (or degradation) and antibacterial properties are exploited by any MoO_3 nanostructures. In view of it, it would be interesting to explore MoO_3 nanostructures.

In this context, we report here that MoO_3 nanoparticle anchored graphene demonstrates the bifunctionality towards dye adsorption and antibacterial activities. The MoO_3-graphene showed excellent direct adsorption of a cationic dye (MB) than an anionic dye methyl orange (MO) compared to pristine graphene and MoO_3. The maximum adsorption capacity of MB by MoO_3-graphene is 625 mg g^{-1}, which is higher than or comparable to some of the activated carbons and mesoporous carbons. The MoO_3-graphene composite also showed antibacterial activity towards both gram-positive and gram-negative bacteria. Therefore, it was commented that MoO_3-graphene acts as a bifunctional agent for water purification.

2. Experimental

MoO_3 nanoparticles were anchored to graphene surface by a simple hydrothermal method. The graphene nanopowder (obtained from Sisco Research Laboratories Pvt. Ltd India) was treated with concentrated HNO_3 for 24 h and washed thoroughly by distilled water. The acid treated graphene (30 mg) was dispersed in 30 ml of distilled water by ultrasonication. Then, 500 mg of $(NH_4)_2MoS_4$ was dissolved in the above solution. The sol was hydrothermally treated at 160 °C for 12 h. The black product after cooling was recovered by centrifugation and washed with deionized water and dried at 110 °C. The dried product was calcined at 350 °C for 3 h in air at a heating rate of 5 °C min^{-1}. Pristine MoO_3 was synthesized by the same protocol without graphene addition. Graphene-MoO_3 nanoparticles and pristine MoO_3 are denoted as G-MoO_3 and MoO_3 respectively.

The materials were characterized by powder x-ray diffraction (Cu-K_α radiation, $\lambda = 1.5418$ Å), transmission electron microscopy (TEM), N_2 adsorption–desorption (BET) isotherms and Fourier transform infrared (FTIR) spectroscopy.

For adsorption of MB from water, 0.02 g of G-MoO_3, MoO_3 and graphene were dispersed into 50 ml of MB solution of different concentrations ranging from 50 to 500 ppm at room temperature. These solutions were stirred continuously. During this process, samples were collected from the solution at different time intervals and the concentration of the dye was determined by UV–visible spectroscopy. The same procedure was adopted for adsorption of MO. The concentrations of MB and MO were analyzed from absorbance at 663 nm and 466 nm wavelength respectively.

The antibacterial activity was evaluated on *Staphylococcus aureus* (Gram-positive bacteria) and *Escherichia coli* (Gram-negative bacteria) by using optical density (OD_{600}) and colony-forming unit experiments on agar plates at different incubation times as described in [43, 44].

3. Results and discussion

The representative TEM images of the investigated materials are shown in figure 1. The images of pristine MoO_3 indicate that they are crystallized in irregular shape and form aggregates (figures 1(b) and (c)). However, while performing the synthesis in presence graphene, MoO_3 crystallized in the form of nanoparticles in the graphene surface as shown in figures 1(d) and (e). Some of the MoO_3 nanoparticles take the shape of nanospindles (figure 1(f)). The MoO_3 nanospindles have typical length and diameter of about 50–100 nm and 10–50 nm respectively. The x-ray diffraction patterns (figure 2(a)) of both MoO_3 and G-MoO_3 can be clearly indexed to α-MoO_3 phase (JCPDS 05-0508). N_2 adsorption/desorption isotherms show BET surface areas of 60 m^2 g^{-1} and 68 m^2 g^{-1} for MoO_3 and G-MoO_3 respectively (figure 2(b)).

The possible growth mechanism is illustrated schematically in figure 3. Initially, $MoS_4{}^{2-}$ subunits from $(NH_4)_2MoS_4$ is expected to graft to the surface functional groups of graphene. Further, the hydrothermal treatment results in the formation of MoS_3 nanocrystallites in the graphene surface as follows: $(NH_4)_2(MoS_4) \rightarrow MoS_3 + 2NH_3 + H_2S$. When the product is heated at 350 °C in air, MoS_3 nanocrystallites oxidized to MoO_3 nanoparticles (figure 3(a)). In absence of graphene, $MoS_4{}^{2-}$ subunits agglomerate themselves to form bulk MoS_3 which in turn converts to bulk MoO_3 (figure 3(b)).

Figure 4(a) shows the adsorption curves of MB, a cationic dye, by G-MoO_3. It is observed that G-MoO_3 rapidly adsorbs MB at lower concentrations (<250 ppm). It reached more than 95% of adsorption within 30 min for 100 and 250 ppm MB. However, the adsorption rate is 35% for 500 ppm MB. It is interesting to note the corresponding UV–visible absorption spectra (figures 4(b)–(d)). For example, the peak at 663 nm immediately vanished while there is emergence of additional broad peak below 400 nm for 70 ppm of MB. This peak intensity increases continuously with adsorption time. For 250 ppm of MB, 663 nm and 292 peaks continuously decreases with time and after 30 min, the broad peak below 400 nm starts evolving. However, this behavior is not observed for 500 ppm of MB. The equilibrium adsorption capacity (q_e) was calculated by

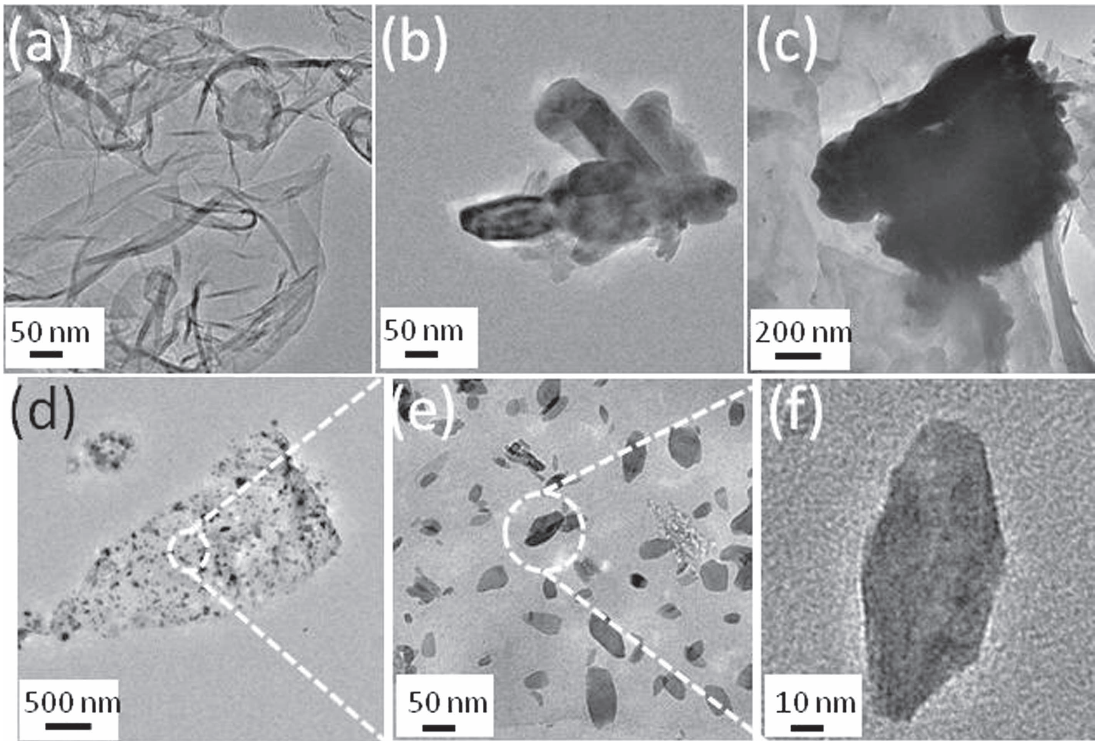

Figure 1. Transmission electron micrographs of (a) graphene, (b) and (c) MoO_3, (d)–(f) G-MoO_3.

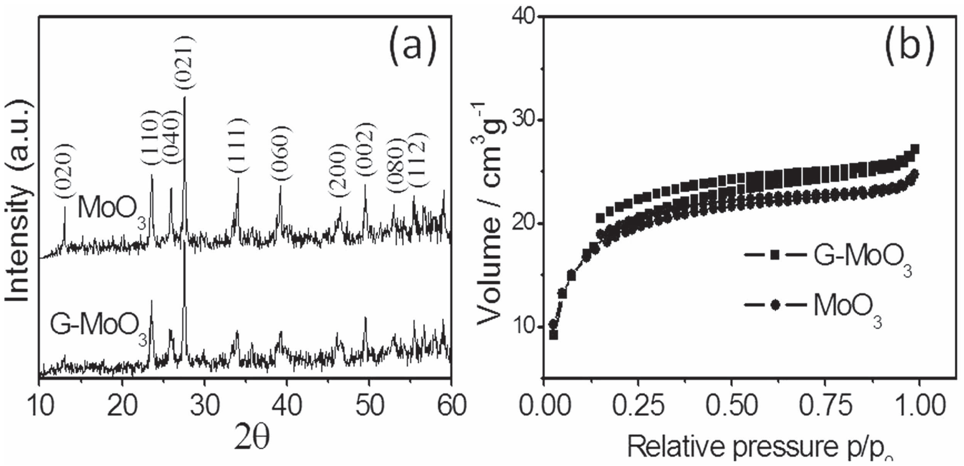

Figure 2. (a) X-ray diffraction patterns and (b) N_2 adsorption–desorption isotherms of G-MoO_3 and MoO_3.

$\left(q_e = \frac{(C_o - C_e)V}{W}\right)$, where C_o is the initial concentration of MB, C_e is the equilibrium concentration of MB, V is the volume of the solution and W is the mass of G-MoO_3 taken in the experiment [12, 13]. Figure 5(a) shows the variation of equilibrium adsorption capacity as a function of the equilibrium concentration of MB in the solution. The absorption data were fitted to Langmuir isotherm model which states that $\frac{C_e}{q_e} = \frac{C_e}{q_m} + \frac{1}{K_2 q_m}$, where K_2 is the Langmuir adsorption constant and q_m is the maximum adsorption capacity [12, 13]. Thus, a plot of $\frac{C_e}{q_e}$ versus C_e should be linear as shown in figure 5(b). The maximum adsorption capacity of MB by G-MoO_3 is evaluated to be 625 mg g^{-1}. These adsorption values are much higher than reported MoO_3 nanostructures [30, 31]. It is also higher than or comparable to some of the activated carbons, mesoporous carbon, carbon nanotubes and graphene [12–17]. Similar high adsorption was shown by WO_3 nanosheets [45]. It indicates that G-MoO_3 possesses excellent adsorption capacities for MB. The absorption data did not follow the Freundlich isotherm model which states that $\text{Ln } q_e = \text{Ln } k_f + \frac{1}{n} \text{Ln } C_e$, where k_f is Freundlich constant and $1/n$ is an empirical parameter [12, 13]. The nonlinearity of Lnq_e versus LnC_e is shown in figure 5(c).

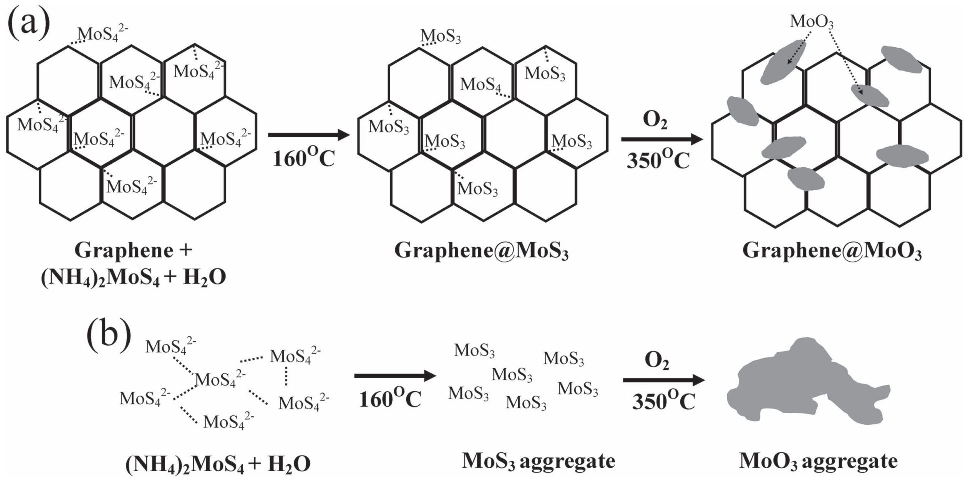

Figure 3. Schematic representation of the growth of (a) G-MoO_3 and (b) pristine MoO_3.

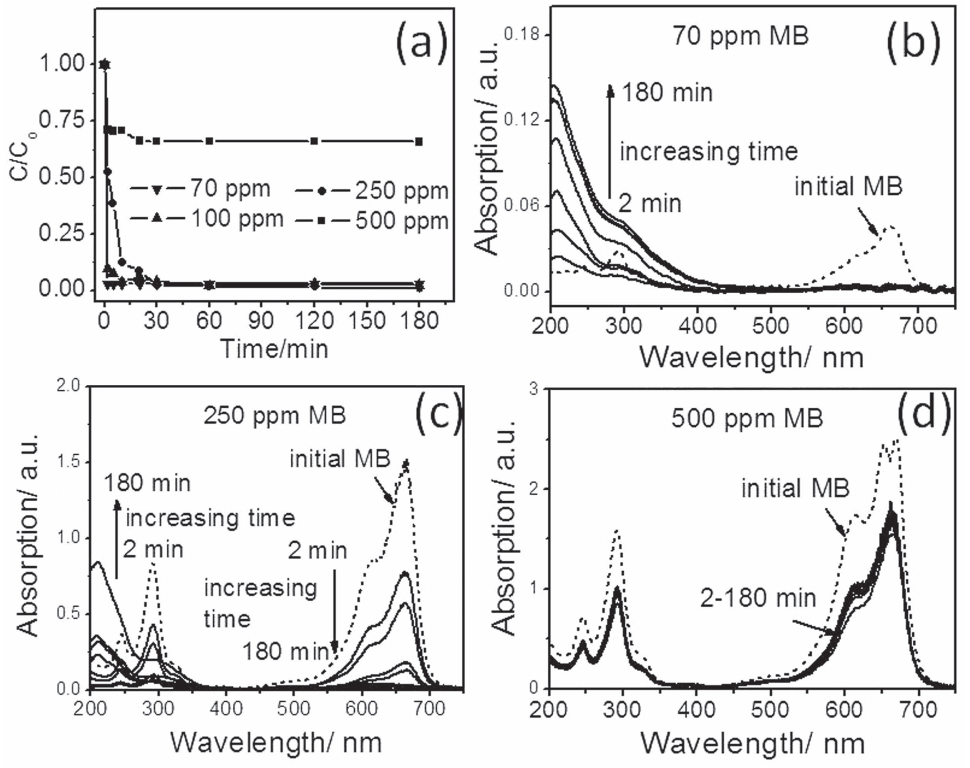

Figure 4. (a) Adsorption rate curves for MB by G-MoO_3, UV–visible absorption spectra of (b) 70 ppm, (c) 250 ppm and (d) 500 ppm of MB at different absorption times with 0.02 g of G-MoO_3.

The kinetics of the adsorption of MB (250 ppm) was also fitted to the pseudo first-order and pseudo second-order kinetic models. The pseudo first-order model is represented by: $\log (q_e - q_t) = \log q_e - \frac{k}{2.303}t$, where k is the rate constant of adsorption, q is the amount of MB adsorbed at time t [12, 13]. The pseudo second-order model is represented by: $\frac{t}{q_t} = \frac{1}{k_2 {q_e}^2} + \frac{t}{q_e}$, where k_2 is the pseudo-second-order rate constant [12, 13]. The linearity of $\frac{t}{q_t}$ versus t (figure 6(b)) is more pronounced than the linearity of $\log (q_e - q_t)$ versus t (figure 6(a)). The correlation coefficient (R^2) values for first-order and second-order fittings are 0.94 and 0.99 respectively. Therefore, it is commented that the adsorption of MB onto G-MoO_3 fits the second-order kinetics.

Figure 7(a) shows the comparison of MB adsorption by G-MoO_3, pristine MoO_3 and graphene. It is apparent that adsorption rate is significantly higher for G-MoO_3 than pristine MoO_3 and graphene. Again, pristine MoO_3 shows better adsorption than graphene. It is noted that the surface areas of G-MoO_3 (68 $m^2\ g^{-1}$)

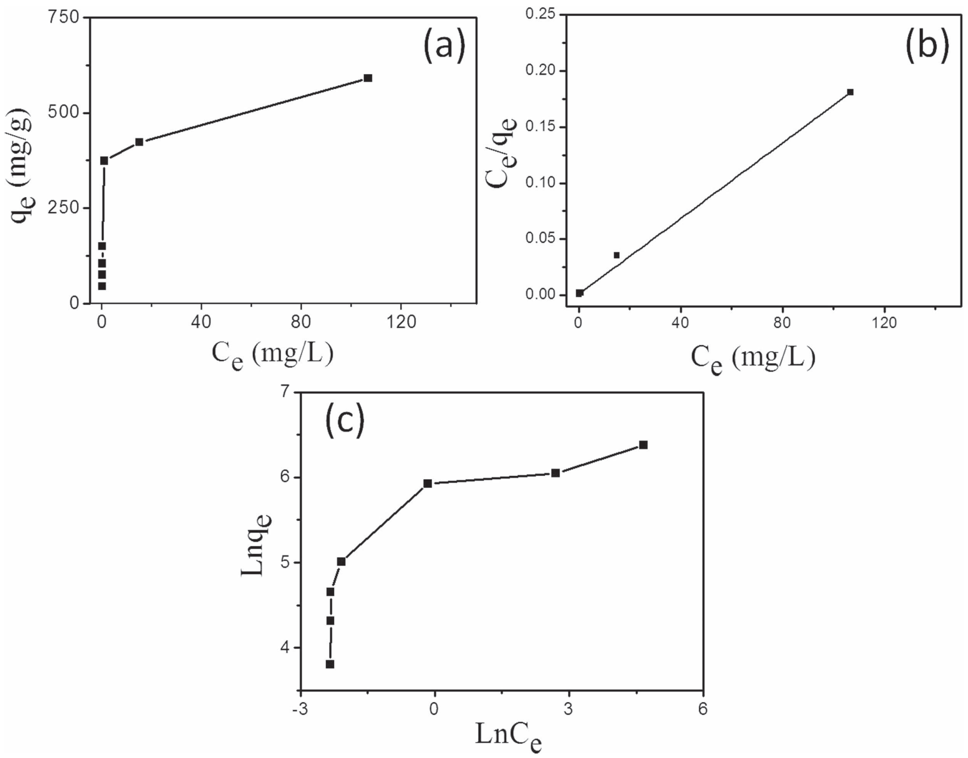

Figure 5. (a) Variation of the adsorption capacity as a function of the equilibrium concentration of MB, (b) Langmuir isotherm and (c) Freundlich isotherm fitting.

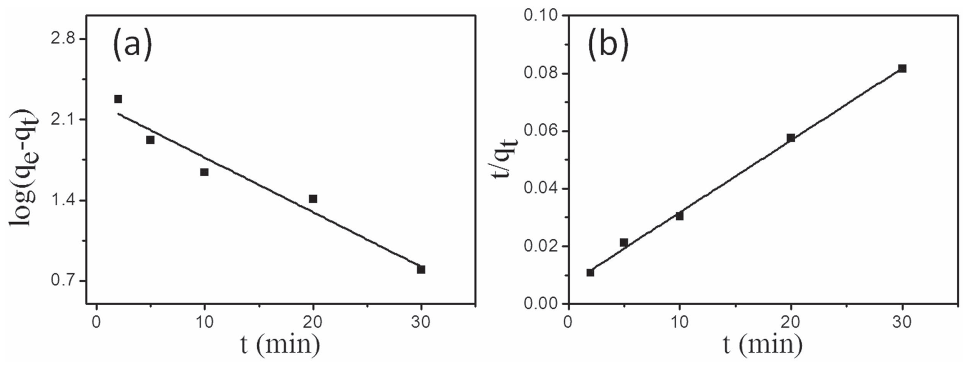

Figure 6. (a) Pseudo first-order kinetic and (b) pseudo-second-order kinetic plots for adsorption of MB (250 ppm) by G-MoO_3.

and MoO_3 (60 m^2 g^{-1}) are almost identical. Therefore, the surface area effect may be ruled out. It is possible that graphene and MoO_3 nanoparticles synergistically work to enhance the adsorption capacity.

Adsorption of MB was also confirmed by FTIR spectra. Figures 7(b) and (c) indicates that new peaks appeared at 1050–1650 cm^{-1} (marked by the dotted box) corresponding to the vibrations of MB molecules after adsorption of MB by G-MoO_3 and MoO_3. It showed that the MB molecules effectively adsorbed on MoO_3 surface. However, no such vibrations of MB can be observed for pristine graphene (figure 7(d)). Therefore, it is expected that graphene acts as a catalyst in enhancing the adsorption capacity of MoO_3.

The graphene-MoO_3 nanoparticles were also employed to adsorb an anionic dye such as MO. However, the UV–visible spectra confirm that G-MoO_3 does not show adsorption of MO (figure 8(a)). It is again supported by the FTIR spectra obtained from G-MoO_3 after the adsorption of MO experiment (figure 8(b)). It suggests that G-MoO_3 shows selective adsorption towards cationic dye.

The antibacterial experiments show that the bacteria cultures achieve growth profiles attaining very low cell concentration of 0.1 OD and 0.7 OD at 12 h incubation for *S. aureus* and *E. coli* respectively with G-MoO_3 at 0.4 mg ml^{-1} concentration (figures 9(a) and (b)). It indicates that the bacterial growth is efficiently inhibited by G-MoO_3. Moreover, the colony forming unit assay of *S. aureus* and *E. coli* showed visible growth efficiency of

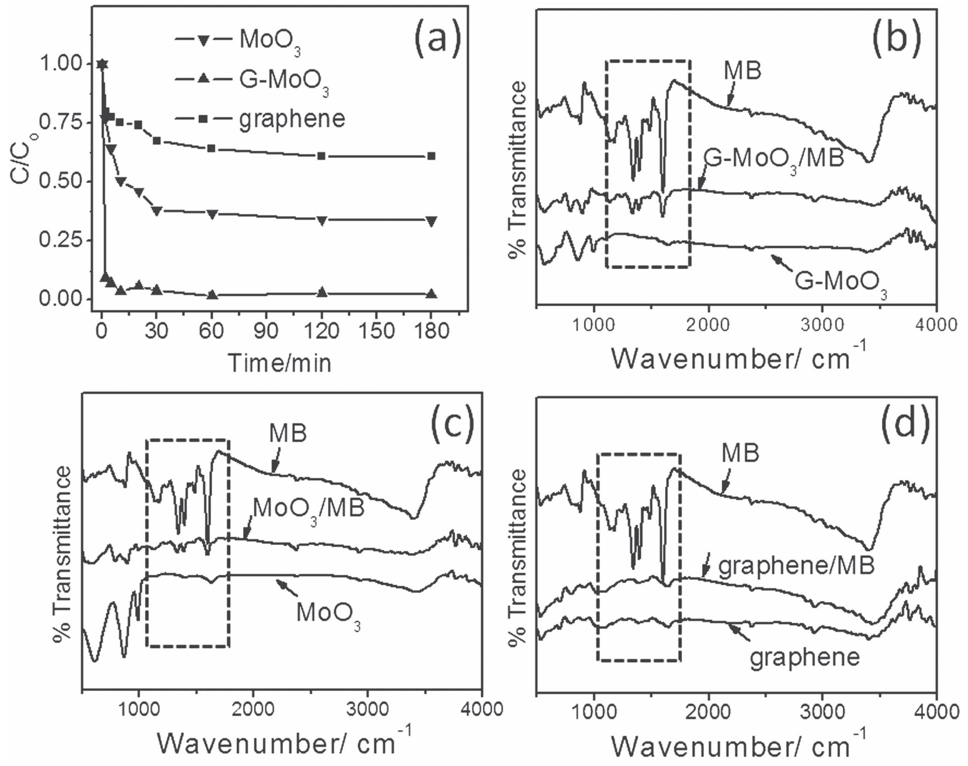

Figure 7. (a) Comparison of adsorption rate curves for 100 ppm MB with graphene, MoO_3 and G-MoO_3, FTIR spectra of (b) G-MoO_3, (c) MoO_3 and (d) graphene before and after MB adsorption.

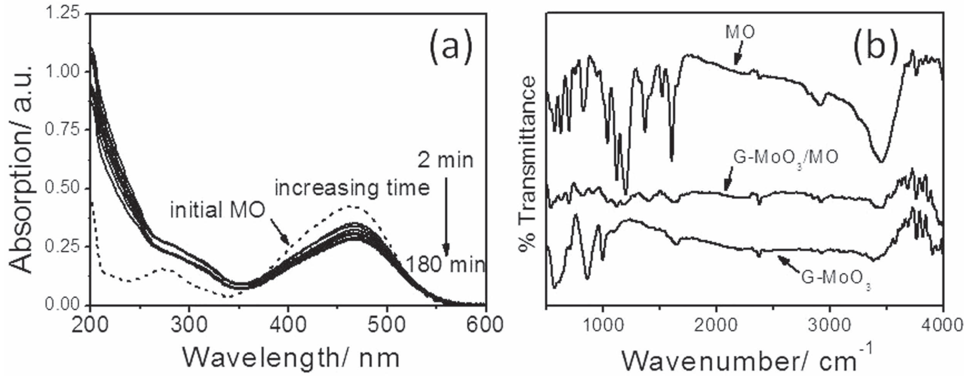

Figure 8. (a) UV–visible absorption spectra of 100 ppm MO at different absorption times with 0.02 g of G-MoO_3 and (b) FTIR spectra G-MoO_3 before and after MO adsorption.

above 90% and 80% respectively at 24 h (figures 9(c) and (d). This observation again demonstrates the bacteriostatic property of G-MoO_3 [43, 44, 46].

The exact adsorption and antibacterial mechanism is not well understood and a more rigorous study is required via XPS, NMR, mass spectroscopy and *in situ*/*ex situ* electron microscopy [47]. However, it may be possible that graphene may induce generation of hydroxyl radicals (·OH) from hydroxyl groups (OH) present in MoO_3 surface. This reactive species in turn reacts with the MB molecule after adsorption on the MoO_3 surface and results in degradation [39, 48–50]. The rate of degradation increases with time and, therefore, the peak intensity below 400 nm increases continuously with time (figures 4(b) and (c)). Again, it is also well known that reactive hydroxyl radicals (·OH) oxidize the bacterial cell membrane [18]. Hence, whenever the bacteria comes in contact with G-MoO_3, it acts as an antibacterial agent due to the presence of hydroxyl radicals (·OH) in the surface of MoO_3. Therefore, it can be anticipated that graphene acts as a catalyst for adsorption and antibacterial activities.

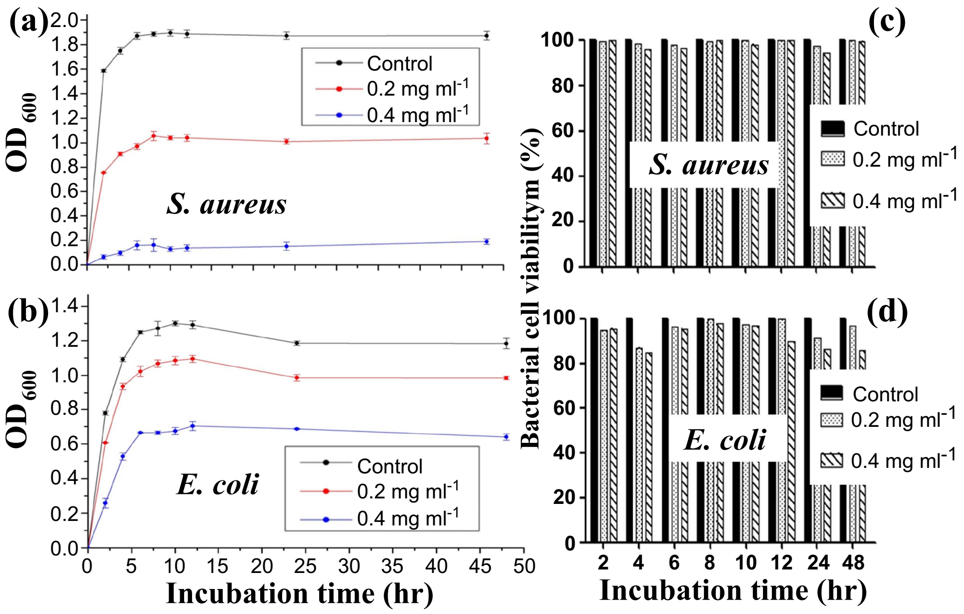

Figure 9. Optical density (600 $_{nm}$) growth profile and cell viability (%) of *S. aureus* (a) and (c) and *E. coli* (b), (d) treated with G-MoO_3 at different incubation times.

4. Conclusion

In summary, a simple hydrothermal method to anchor MoO_3 nanoparticles in graphene is described. The nanocomposite demonstrated excellent adsorption of a cationic dye (MB) than an anionic dye (MO). It shows fast adsorption up to 250 ppm of MB within 30 min. The maximum adsorption capacity of MB is 625 mg g^{-1}. Again, the graphene-MoO_3 nanoparticles can serve as an antibacterial agent to inhibit the multiplication of bacteria cells in water due to the bacteriostatic nature. Therefore, it is termed that graphene-MoO_3 nanoparticles act as a bifunctional agent for water purification.

Acknowledgment

SKD thanks the financial support from Science and Engineering Research Board, Department of Science and Technology, Government of India (Grant No.: YSS/2015/000765)

References

[1] Hao Z and Iqbal A 1997 *Chem. Soc. Rev.* **26** 203
[2] Zollinger H 2003 *Color Chemistry: Synthesis, Properties and Applications of Organic Dyes and Pigments* 3rd revised edn (New York: VCH)
[3] Robinson T, McMullan G, Marchant R and Nigam P 2001 *Bioresour. Technol.* **77** 247
[4] Linak E, Fink U, Kishi A and Guan M 2014 *Chemical Economics Handbook* (Dyes, ISH)
[5] Ghaly A E, Ananthashankar R, Alhattab M and Ramakrishnan V V 2014 *J. Chem. Eng. Process Technol.* **5** 1000182
[6] Qu X, Alvarez P J J and Li Q 2013 *Water Res.* **47** 3931
[7] Sanghi R and Bhattacharya B 2002 *Color Technol.* **118** 256
[8] Zhu T, Chen J S and Lou X W 2012 *J. Phys. Chem.* **116** 6873
[9] Xu C, Wang Y, Zhao P, Chen H and Liu Y 2015 *Mater. Lett.* **159** 64
[10] Wang X, Ding J, Yao S, Wu X, Feng Q, Wang Z and Geng B 2014 *J. Mater. Chem.* **2** 15958
[11] Liu B X, Wang J S, Wu J S, Li H Y, Li Z F, Zhou M L and Zuo T Y 2014 *J. Mater. Chem.* **2** 1947
[12] Ramesha G K, Kumara A V, Muralidhara H B and Sampath S 2011 *J. Colloid Interface Sci.* **361** 270
[13] Liu T *et al* 2012 *Colloids Surf.* B **90** 197
[14] Attia A A, Rashwan W E and Khedr S A 2006 *Dyes Pigments* **69** 128
[15] Wang S B, Zhu Z H, Coomes A, Haghseresht F and Lu G Q 2005 *J. Colloid Interface Sci.* **284** 440
[16] Li J T, Li B L, Wang H C, Bian X B and Wang X M 2011 *Carbon* **49** 1912
[17] Khoerunisa F *et al* 2012 *J. Phys. Chem.* C **116** 11216
[18] Oveisi H, Rahighi S, Jiang X, Nemoto Y, Beitollahi A, Wakatsuki S and Yamauchi Y 2010 *Chem. Asian J.* **5** 1978
[19] Dutta D P, Singh A, Ballal A and Tyagi A K 2014 *Eur. J. Inorg. Chem.* **33** 5724
[20] Roca R A *et al* 2015 *Catal. Sci. Technol.* **5** 4091
[21] Balendhran S, Walia S, Nili H, Ou J Z, Zhuiykov S, Kaner R B, Sriram S, Bhaskaran M and Kalantar K 2013 *Adv. Funct. Mater.* **23** 3952
[22] Wang C, Irfan I, Liu X and Gao Y 2014 *J. Vac. Sci. Technol.* **32** 040801
[23] Noerochim L, Wang J Z, Wexler D, Chao Z and Liu H K 2013 *J. Power Sources* **228** 198

[24] Yang X, Ding H, Zhang D, Yan X, Lu C, Qin J, Zhang R, Tang H and Song H 2011 *Cryst. Res. Technol.* **46** 1195
[25] Cao X, Zheng B, Shi W, Yang J, Fan Z, Luo Z, Rui X, Chen B, Yan Q and Zhang H 2015 *Adv. Mater.* **27** 4695
[26] Yang X, Lu C, Qin J, Zhang R, Tang H and Song H 2011 *Mater. Lett.* **65** 2341
[27] Zhou J, Song J, Li H, Feng X, Huang Z, Chen S, Ma Y, Wang L and Yan X 2015 *New J. Chem.* **39** 8780
[28] Yang X, Tang H, Zhang R, Song H and Cao K 2011 *Cryst. Res. Technol.* **46** 409
[29] Zheng L, Xu Y, Jin D and Xie Y 2009 *Chem. Mater.* **21** 5681
[30] Ma Y, Jia Y, Jiao Z, Wang L, Yang M, Bi Y and Qi Y 2015 *Mater. Lett.* **157** 53
[31] Wang M, Song X, Cheng X L, Zhou X, Zhang X, Cai Z, Xu Y M, Gao S, Zhao H and Huo L H 2015 *RSC Adv.* **5** 85248
[32] Cheng L, Shao M, Wang X and Hu H 2009 *Chem. Eur. J.* **15** 2310
[33] Chen Y, Lu C, Xu L, Ma Y, Hou W and Zhu J J 2010 *Cryst. Eng. Commun.* **12** 3740
[34] Chithambararaj A, Sanjini N S, Velmathi S and Bose A C 2013 *Phys. Chem. Chem. Phys.* **15** 14761
[35] Zhou Y F *et al* 2015 *Mater. Lett.* **154** 132
[36] Zhong M, Wei Z, Meng X, Wu F and Jingbo L 2014 *Eur. J. Inorg. Chem.* **20** 3245
[37] Rakkesh A R and Balakumar S 2015 *J. Nanosci. Nanotechnol.* **15** 4316
[38] Chithambararaj A, Winston B, Sanjini N S, Velmathi S B and Chandra A 2015 *J. Nanosci. Nanotechnol.* **15** 4913
[39] Manivela A, Lee G J, Chen C Y, Chen J H, Mac S H, Horng T L and Wu J J 2015 *Mater. Res. Bull.* **62** 184
[40] Krishnamoorthy K, Premanathan M, Veerapandian M and Kim S J 2014 *Nanotechnology* **25** 31510
[41] Krishnamoorthy K, Veerapandian M, Yun K and Kim S J 2013 *Colloid Surf.* B **112** 521
[42] Zollfrank C, Gutbrod K, Wechsler P and Guggenbichler J P 2012 *Mater. Sci. Eng.* C **32** 47
[43] Erb T J, Kiefer P, Hattendorf B, Gunther D and Vorholt J A 2012 *Science* **337** 467
[44] Yu L, Zhang Y T, Zhang B and Liu J D 2014 *Sci. Rep.* **4** 4551
[45] Luo J Y, Cao Z, Chen F, Li L, Lin Y R, Liang B W, Zeng Q G, Zhang M, Hea X and Li C 2013 *Appl. Surf. Sci.* **287** 270
[46] Cosgrove S E 2006 *Clin. Infectious Diseases* **42** 82
[47] Wang X, Mei L, Xing X, Liao L, Lv G, Li Z and Wu L 2014 *Appl. Catal.* B **160** 211
[48] Houas A, Lachheb H, Ksibi M, Elaloui E, Guillard C and Herrmann J M 2001 *Appl. Catal.* B **31** 145
[49] Huang G, Zhang C, Long Y, Wynn J, Liu Y, Wang W and Gao J 2013 *Nanotechnology* **24** 395601
[50] Oliveira L C A, Gonçalves M, Guerreiro M C, Ramalho T C, Fabris J D, Pereira M C and Sapag K 2007 *Appl. Catal.* A **316** 117